01,05

High-entropy FeCoNiP-Me alloys (Me = Zn, Zr, W), made by chemical deposition

© E.A. Denisova[1], L.A. Chekanova[1], S.V. Komogortsev[1,2], I.G. Vazhenina[1], R.S. Ishakov[1], D. Koh[3], D.A. Velikanov[1], G.N. Bondarenko[1,4], I.V. Nemtsev[1,3]

[1] Kirensky Institute of Physics, Federal Research Center KSC SB, Russian Academy of Sciences, Krasnoyarsk, Russia
[2] Siberian State University of Science and Technology, Krasnoyarsk, Russia
[3] Federal Research Center „Krasnoyarsk Scientific Center of the Siberian Branch of the Russian Academy of Sciences“, Krasnoyarsk, Russia
[4] Institute of Chemistry and Chemical Technology, Federal Research Center KSC SB RAS, Krasnoyarsk, Russia

E-mail: len-den@iph.krasn.rujoe

Received April 18, 2024
Revised April 18, 2024
Accepted May 8, 2024

The results of a study of the microstructure and magnetic properties of nanostructured coatings made of high entropy FeCoNi(P)-Me (Me = Zn, Zr, W) alloys synthesized by chemical deposition are presented. The phase-structural state of the coatings has been studied by X-ray diffraction and electron microscopy. The magnetic characteristics of the synthesized materials (saturation magnetization, coercive force, local anisotropy fields) were studied as functions of the Zn, Zr, or W content in the FeCoNi(P)-Me alloy. The magnetic properties are discussed within the framework of the random magnetic anisotropy model. The boundary values of entropy and enthalpy of mixing have been determined, which contribute to the formation of an unordered solid solution in the production of high-entropy alloys based on FeCoNi(P) by chemical precipitation.

Keywords: high-entropy alloys, coatings based on FeCoNi(P), chemical deposition, magnetic properties, entropy of mixing.

DOI: 10.61011/PSS.2024.07.58964.43HH

1. Introduction

The conventional approaches to development of new alloys (based on selection of alloying elements to obtain the required functional characteristics of the alloy) and technologies have already reached the ceiling and will not lead to a brand new improvement of its properties. The technologies of products fabrication in general doesn't allow for specifics of phase formation, multilayer structure, scale and distribution of structural elements which often cannot provide optimal combination of magnetic and mechanical properties. Currently, the interest is focused on the so called high-entropy alloys (HEA) defined as alloys containing at least five basic elements (each with concentrations 5−35 at.%) [1,2]. Due to some properties characteristic for various HEA types these materials can be considered as perspective for use in electronics, magnito-optics, VHF devices [3,4]. Such multi-component alloys are characterized by high mixing entropy, strong lattice distortions, low diffusion compared to conventional alloys with one basic element [1,5]. High mixing entropy preventing formation of intermetallic phases in HEA and contributing to formation of disordered solid solutions according to many authors [2–7] is a factor leading to a combination of strength and functional properties of the alloys. Magnetic HEA based on FeCoNi with various additional elements Pt or Pd [8], AlCu [9], MnCu [10] combine high corrosion resistance, strength and/or hardness, wear resistance and non-retentive properties. Base alloy FeCoNi is featuring high magnetization saturation (160 emu/g), minimal coercive force, however, low electric resistance greatly reduces the potential of its application as a shielding surface. Electrical resistance can be enhanced practically by an order when transiting to the amorphous phases (e.g., by adding some amorphous additives like P or Zr) or to HEA [11]. It was found [8,12,13] that magnetic properties of FeCoNi based alloys greatly depend on the type of additives. Thus, the additives Cr lead to paramagnetic state of the alloy at room temperature, adding of Al in FeCoNiCr alloy results in drastic Curie temperature rise up to 600 K [14]. Our study was focused on modification of magnetic properties of FeCoNi(P) alloy when adding additional components Zn, Zr and W. In most cases the high entropy alloys are obtained by melting of elements followed by crystallization of the total melt, thermal sputtering; mechanical melting of individual element powders in planetary ball mils is often used [15–19]. It was discovered earlier that alloys of the same chemical composition obtained by various methods are characterized by different microstructure and, hence, different properties [20]. As seen from multiple studies of the multi-component alloys no such combination of factors yet has been found that could enable to forecast the micro-

structure, and, therefore, the material properties, with high degree of reliability.

This paper describes the experimental results of studying the influence of such elements as Zn, Zr and W on the microstructure and magnetic characteristics of alloys FeCoNi(P)-*Me* ($Me = $ Zn, Zr, W) produced by chemical deposition method.

2. Experiment

Three series of coatings $[(FeCoNi)_{95}P_5]_{100-x}Me_x$ $(0 < x < 22)$ $Me = $ Zn (series *A*); $Me = $ Zr (series *B*); $Me = $ W (series *C*) were obtained by the method of chemical deposition on copper and glass substrates based on reaction of metals reduction from aqueous solutions of corresponding salts [21]. The base solution for coatings deposition included salts of metals (cobalt sulfates $CoSO_4$, nickel $NiSO_4$, Mohr salt $Fe(NH_4)_2(SO_4)$; as complexing additives — sodium citrate ($Na_3C_6H_5O_7$) and ammonium sulfate ($(NH_4)_2SO_4$); sodium hypophosphite as a reducing agent (NaH_2PO_2). For deposition of *A* series coatings Zn ($ZnCl_2$) salt was added to the base solution, for coatings of *B* series — Zr ($ZrSO_4$) salt was added, for *C* series coatings — sodium tungstate ($Na_2W_2O_7$) was added. The deposition was carried out at 80°C and the pH value was maintained by adding NaOH solution. The method of metal coatings chemical deposition using hypophosphite has some peculiarities. Along with reduction of metal a reaction of hypophosphite reduction to elemental phosphorous also takes place. Thus, a phosphorous admixture is always present in the obtained metallic deposits. Coatings with a thickness from 0.6 to 5 μm were obtained.

Synthesized samples were studied by electron microscopy (S5500 and TM3000 Hitachi scanning microscopes with an attachment for energy-dispersive analysis) and X-ray diffraction (DRON 3). The chemical composition of the samples was determined by the method of energy-dispersive analysis. The temperature and field dependences of the magnetization were measured on a vibrating magnetometer [22]. Magnetic characteristics of synthesized materials (saturation magnetization M_s, exchange interaction constant *A*, coercive force H_c, local anisotropy field H_a) were studied as functions of Zn, Zr or W concentrations in the alloy FeCoNi(P)-*Me*. The characteristics of the magnetic microstructure — the magnitude of the local anisotropy field, the correlation radius of this anisotropy (R_c), the stochastic domain anisotropy field ($\langle H_a \rangle$) were determined by correlation magnetometry [23].

3. Results and discussion

3.1. Experimental results

The varied composition of the chemical bath for chemical deposition of metals allowed synthesizing a high-entropy alloy coating based on FeCoNi(P) with homogeneous distribution of elements Zn or Zr or W (EDX charts of elements distribution are illustrated in Figure 1), various surface morphology, texture and grain size.

Figure 1 shows SEM-images of coating surfaces for a group of studied samples and cross-sections of FeCoNi(P)-Zn coatings with different Zn concentration. The surface of FeCoNi(P) coatings with W (Figure 1, *a*) and Zr (Figure 1, *c*) as additional elements is arranged as a „cauliflower“ structure, the particles of 150 ÷ 250 nm size are collected in conglomerates with an average size of $\sim 1\,\mu$m. The surface of FeCoNi(P)-Zn coatings (Figure 1, *b*) is characterized by homogeneous filling with spherical grains 120−200 nm. The studies of the transverse cuts showed that coatings with Zn up to 7 at.% have columnar structure (Figure 1, *d*). Coating with zinc content Zn 22 at.% is practically uniform across thickness (Figure 1, *e*).

X-ray diffraction patterns of coatings with various content of Zn and Zr are shown in Figure 2. According to X-ray diffraction data the films and coatings of *A* and *C* series are a nanocrystalline BCC solid solution for all studied concentrations of additional elements. The size of the coherent scattering region, calculated by the Scherrer formula varied within 10−20 nm. The coatings of alloy $[(FeCoNi)_{95}P_5]_{100-x}Zn_x$ $(0 < x < 8)$ are featuring a clearly distinct texture in direction [211].

The crystalline lattice parameter with the increase of Zn concentration is changed in accordance with Vegard rule (see insert window in Figure 2, *a*), thus, proving the formation of a series of solid solutions. For *B* series, the rise of Zr concentration to 7% leads to partial amorphization of alloy $[(FeCoNi)_{95}P_5]_{100-x}Zr_x$, with Zr concentration above 15 at% the alloys of *B* series are X-ray amorphous (Figure 2, *b*). It should be noted that on the diffraction patterns of samples in all series the peaks corresponding to Fe, Co and Ni phosphides are not observed.

The low-temperature behavior of the saturation magnetization M_s in the coatings complies with Bloch's law $T^{3/2}$: $M_s(T) = M_{s0} \cdot (1 - B \cdot T^{3/2})$, which allowed us to estimate the exchange constant as

$$A = \frac{k_B}{8\pi}\left(\frac{M_{s0}}{g\mu_B}\right)^{1/3}\left(\frac{2.612}{B}\right)^{2/3}.$$

The values of saturation magnetization and exchange constant correlate with the quantity of additional element in the alloy, thus, with the increase of Zn concentration in alloy $[(FeCoNi)_{95}P_5]_{100-X}Zn_X$ from 2 to 22 at.% the values M_s decrease from 1200 Gs to 760 Gs, values *A* decrease from $6.3 \cdot 10^{-7}$ to $4.5 \cdot 10^{-7}$ erg/cm. Such monotonous decrease of the exchange constant confirms the fact that a solid solution [24] is formed in the studied high-entropy alloys.

The study of law of magnetization approximation to saturation allowed defining the values of local anisotropy fields, radii of correlation of this anisotropy, anisotropy fields of stochastic domain for the coatings of all of the studied samples groups. Figure 3 shows typical experimental hysteresis loops for FeCoNi(P) based alloys with Zn as an additional element, as well as concentration dependencies of the local anisotropy fields and coercive force. The curves

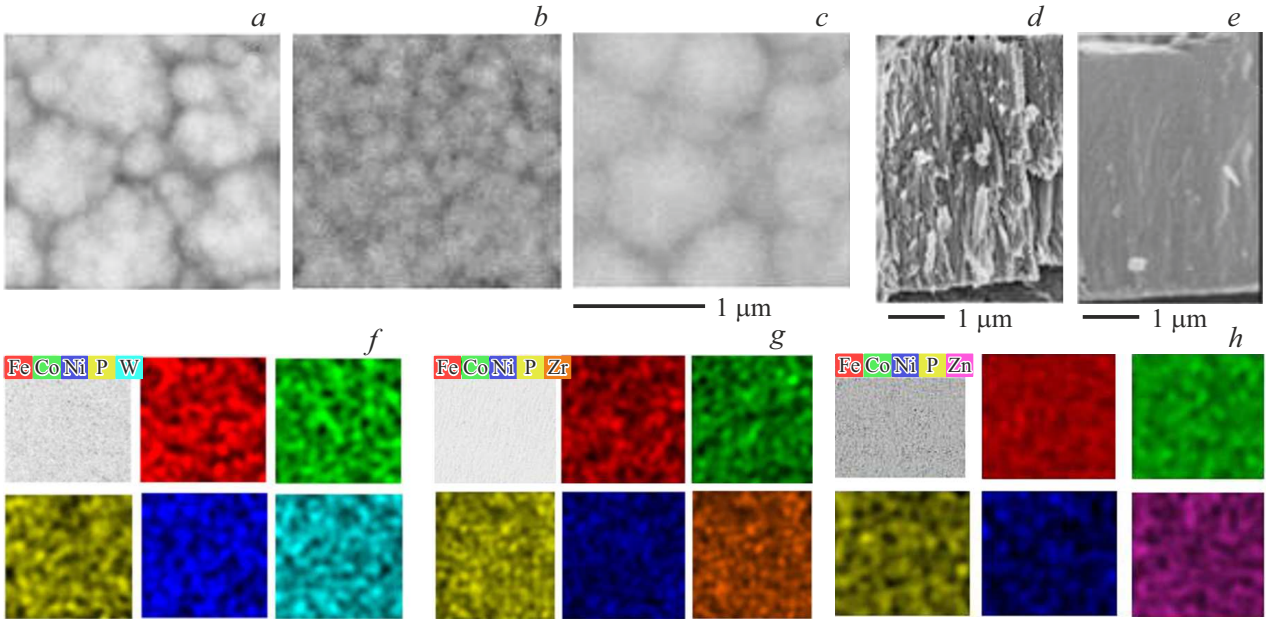

Figure 1. SEM-images of FeCoNi(P) surface coatings obtained with various additional elements: W (a), Zn (b) and Zr (c); and images of cross-sections of coatings $[(FeCoNi)_{95}P_5]_{100-x}Zn_x$ with $x = 2$ (d) and $x = 22$ (e). Elements distribution charts for the alloys of series A (f), B (g) and series C (h).

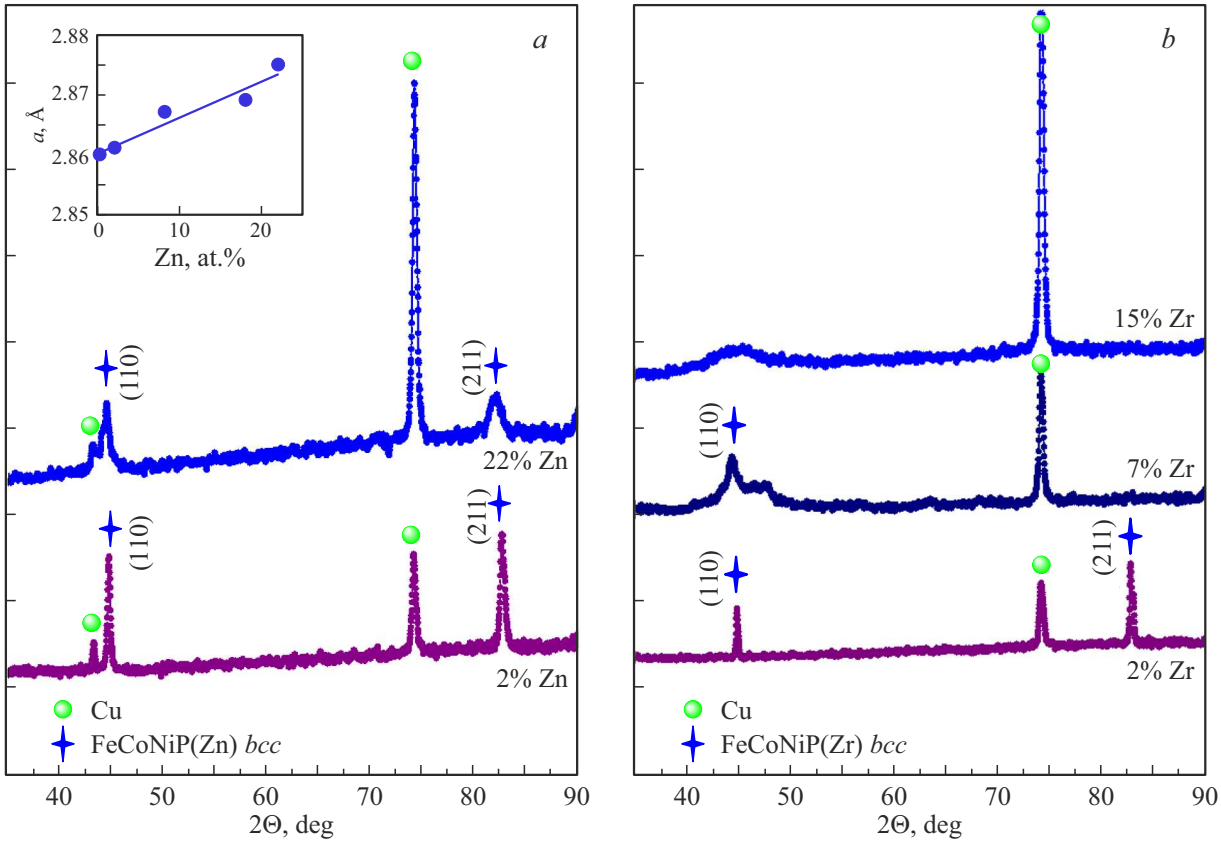

Figure 2. Diffraction patterns of coatings FeCoNi(P)-*Me* with $Me = Zn$ (a) and $Me = Zr$ (b). The figure shows the dependence of the lattice parameter of BCC of a solid solution on Zn content.

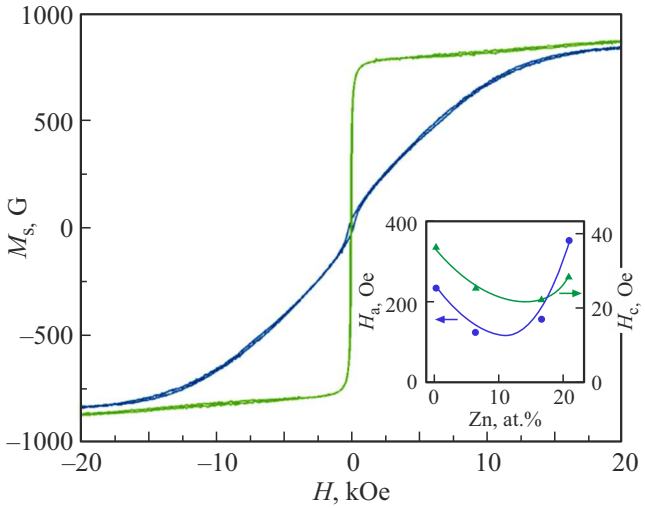

Figure 3. Hysteresis loops for alloy $[(FeCoNi)_{95}P_5)_{82}Zn_{18}$ measured perpendicular and parallel to the film surface. The insert window in figure illustrates concentration dependencies of local anisotropy field and coercive force for alloy of A series.

of magnetization approximation to saturation in all series of coatings for all values x are characterized by the Akulov dependence $M(H) \propto H^{-2}$ in fields larger than 2−6 kOe, which allowed to calculate for these alloys the value of the rms fluctuation of the local magnetic anisotropy field aH_a ($H_a = 2K/M_s$ — the local magnetic anisotropy field, the coefficient a — the symmetrical numerical coefficient for uniaxial anisotropy equal to $a = 1/15^{1/2}$, for cubic — $a = (2/105)^{1/2}$. Values H_a vary from 0.5 to 1 kOe for the samples of series C, from 0.1 to 0.4 kOe for samples of series A and B. In the range 1−3 kOe, magnetization approximation to saturation looks as $M(H) \propto H^{-\alpha}$. The index of degree α is related to the effective dimensionality of the magnetic microstructure in a given field range. The magnitude of the field at which the power dependence change $H_R = 2A/MR_c^2$ occurs allows to estimate the magnitude of the correlation radius of the random anisotropy R_c. Values R_c lie within the range 6−22 nm for all coating series. It was found that the lowest coercive force of 20 Oe is reached at highest values of $R_c \sim 22$ nm.

3.2. Analysis of thermodynamic parameters of high-entropy alloys FeCoNi(P)-*Me* (*Me* = Zn, Zr, W)

Let's analyze the results obtained using Hume-Rothery rules, and from approaches applied in papers [1,2,4–6,16,25]. For high-entropy alloys the decisive factors for the formation of solid solution or amorphous phase in elements melting are the mixing entropy ΔS_{mix}, mixing enthalpy ΔH_{mix}, difference in sizes of atoms δ. The authors of papers (e. g., [25,26]) take into account the Pauling electronegativity difference $\Delta\chi$ and the concentration of valence electrons per atom VEC. The values of configuration mixing entropy ΔS_{mix}, mixing enthalpy ΔH_{mix}, difference in atoms sizes δ and Pauling electronegativity $\Delta\chi$ are traditionally calculated by the following formulae [1,6,7]:

$$\Delta S_{mix} = -R\sum_{i=1}^{n} c_i \ln c_i, \tag{1}$$

where c_i — content of i element in atomic percentage, R — universal gas constant; standard mixing enthalpy through Miedema method:

$$\Delta H_{mix} = \sum_{i=1, i\neq j}^{n} \Omega_{ij} c_i c_j, \tag{2}$$

where $\Omega_i j = 4\Delta_{mix}^{AB}$ — parameter of interaction between i and j elements in the solution, Δ_{mix}^{AB} — mixing enthalpy of binary alloy AB, we used the values of mixing enthalpy of binary alloys from paper [27]; the difference of elements atom radii can be defined as

$$\delta = 100\sqrt{\sum_{i=1}^{n} c_i\left(1 - r_i/\bar{r}\right)^2}, \tag{3}$$

where $\bar{r} = \sum c_i r_i$, r_i — atom radius of i element; the electronegativity difference is defined in compliance with classic Hume-Rothery rule:

$$\Delta\chi = \sqrt{\sum_{i=1}^{n} c_i(\chi_i - \bar{\chi})^2}, \tag{4}$$

where $\bar{\chi} = \sum c_i\chi_i$, χ — Pauling electronegativity difference; the concentration of valence electrons per atom is defined as

$$\mathrm{VEC} = \sum_{i=1}^{n} c_i \mathrm{VEC}_i, \tag{5}$$

where VEC_i — concentration of valence electrons per atom for i element.

The alloy entropy is defined by the value of four components: configuration mixing entropy (ΔS_{mix}), atoms oscillations entropy (ΔS_v), electrons motion entropy (ΔS_e) and entropy of magnetic moments (ΔS_m). However, in the multi-component alloys the configuration entropy greatly exceeds the contribution of other components ΔS_v, ΔS_m and ΔS_e [5]. It is suggested [1,4,25] that a solid solution in manufacture of high-entropy alloys will be formed if the above-mentioned parameters lie within the range: $\delta < 8.5$, $11 < \Delta S_{mix} < 19.5$ J/(K · mol), — $22 < \Delta H_{mix} < 7$ kJ/mol, formation of amorphous phase is observed at $-40 < \Delta H_{mix} < -5.5$ kJ/mol, $7 < \Delta S_{mix} < 14$ J/(K · mol), $\delta > 9$. Values ΔS_{mix}, ΔH_{mix}, δ, $\Delta\chi$ and VEC for the studied alloys calculated by formulae (1)−(5) are given in the table. For greater clarity Figure 4 illustrates the data on the influence of ΔS_{mix}, ΔH_{mix} and δ on the phases of coatings of the studied alloys. Values ΔS_{mix} are given for comparison for alloys obtained by casting, deposition and mechanical fusion [25,28–30]. The

Thermodynamic parameters for alloys FeCoNi(P)-*Me* with various content of additional elements

Samples		ΔH_{mix}, kJ/mol	ΔS_{mix}, J/(K · mol)	δ	$\Delta\chi$	VEC	Structure
Series *A*	2% Zn	−8	9	3.7	0.11	8.3	BCC SS
	22% Zn	−4.5	10	5.9	0.11	9	BCC SS
Series*B*	2% Zr	−10	9.6	5.5	0.11	8.5	BCC SS
	7% Zr	−23	9.8	8.5	0.17	8.9	Amorf. + BCC SS
	20% Zr	−23.8	10.4	11	0.23	8	Amorphous
Series *C*	5% W	−5.5	10.3	3.4	0.12	8.5	BCC SS

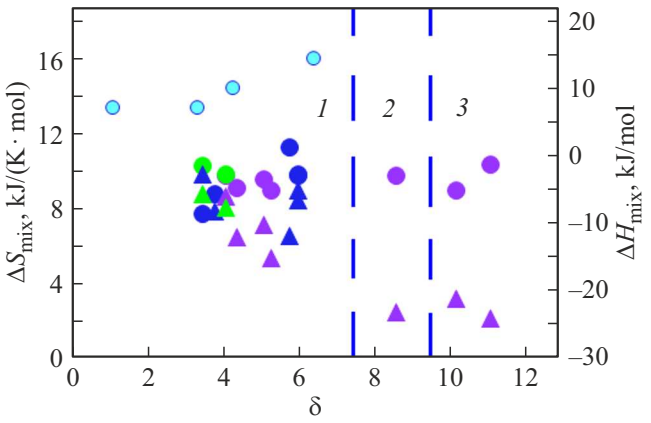

Figure 4. Influence of major factors ΔS_{mix} (circles), ΔH_{mix} (triangles), δ on phase composition of HEA coatings. The alloys of *A* series are designated by blue symbols, alloys of *B* series are designated by violet symbols, alloys of *C* series are designated by green symbols, blue circles indicate data from papers [25,28–30]. In area *1* the BCC SS is formed, in area *2* — a mix of amorphous phase and BCC SS, region *3* — amorphous phase.

phase plane can be divided in three regions, i. e., the first region is a region where disordered BCC of solid solutions (SS) are formed, the second region is the region where BCC of SS and amorphous phase are co-existing, in the third region the studied alloys are X-ray amorphous. For all kinds of alloys the values $\Delta\chi$ comply with Hume-Rothery rule in terms of electronegativity difference for the formation of a substitutional solid solution ($\Delta\chi < 0.4$) In contrast to papers [29,30], where values VEC define the type of the solid solution being formed (FCC- or BCC-type), for all series alloys studied in this paper the values VEC have no decisive influence. The values ΔH_{mix} for samples of all series in all regions are consistent with the data obtained in other papers [3,25–31], i. e. lie within the interval of values where a single-phase solid solution may be produced. If HEA is produced by non-equilibrium method of chemical deposition the single-phase solid solution is formed at lower values of mixing entropy $\Delta S_{mix} \sim 9\,\mathrm{J/(K \cdot mol)}$, compared to methods of casting, sputtering or mechanical fusion for fabrication of the high-entropy alloys.

4. Conclusion

Chemical deposition was used to obtain the high-entropy alloy coatings $(\mathrm{FeCoNi(P)})_{100-x}Me_x$ ($Me = $ Zn, Zr, W) ($0 < x < 22$) with a thickness from 0.6 to 5 μm. The influence of chemical and phase composition of the coatings on the microstructure and magnetic characteristics of the synthesized samples was studied. A comparative analysis was performed to study the magnetic properties of coatings made of FeCoNi(P) high-entropy alloys synthesized using Zn, Zr or W as additional elements. It was demonstrated that magnetization saturation and exchange constant values correlate with the amount of additional element in the alloy. The obtained alloys are distinguished by high saturation inductance (750−1200 G). The field of coatings local anisotropy when using W as an additional element exceeds the equivalent characteristic of FeCoNi(P)-Zn and FeCoNi(P)-Zr alloys.

The paper describes the values ΔS_{mix}, ΔH_{mix}, differences in atomic sizes of alloys elements when the BCC of solid solution or amorphous phase in coatings is observed. It was found that a single-phase solid solution in alloys $(\mathrm{FeCoNi(P)})_{100-x}Me_x$ ($Me = $ Zn, Zr, W) is formed at lower mixing entropy $\Delta S_{mix} \sim 9\,\mathrm{J/(K \cdot mol)}$ compared to conventional methods of high-energy alloys fabrication due to a non-equilibrium nature of chemical deposition method.

Funding

The work was carried out within the framework of the scientific subject of the State Task of the Institute of Physics named after L.V. Kirensky of the Russian Academy of Sciences — an individual branch of FRC of the Krasnoyarsk Scientific Center of Siberian branch of the Russian Academy of Sciences. The authors thank the Krasnoyarsk Regional Research Equipment Sharing Center of the Federal Research Center Krasnoyarsk Science Center of the Siberian Branch of the Russian Academy of Sciences for the provided equipment for measurements.

Conflict of interest

The authors declare that they have no conflict of interest.

References

[1] J.W. Yeh, S.K. Chen, S.J. Lin, J.Y. Gan, T.S. Chin, T.T. Shun, C.H. Tsau, S.Y. Chang. Adv. Eng. Mater. **6**, 299 (2004).
[2] B. Cantor, I.T.H. Chang, P. Knight, A.J.B. Vincent. Mater. Sci. Eng. A**375**–**377**, 213 (2004).
[3] Z. Bataeva, A. Ruktuev, I. Ivanov, A. Yurgin, I. Bataev Obrabotka metallov **23**, *2*, 116 (2021). (in Russian).
[4] A.S. Rogachev. Fizika metallov i metallovedenie **121**, *8*, 807 (2020). (in Russian).
[5] D.B. Miracle, O.N. Senkov. Acta Mater. **122**, 448 (2017).
[6] Y. Zhang, Y.J. Zhou, J.P. Lin, G.L. Chen, P.K. Liaw. Adv. Eng. Mater. **10**, 534 (2008).
[7] V.F. Gorban', N.A. Krapivka, S.A. Firstov. Fizika metallov i metallovedenie **118**, *10*, 1017 (2017). (in Russian).
[8] J. Kitagawa. J. Magn. Magn. Mater. **563**, 170024 (2022).
[9] R. Zheng, Z. Wu, M. Chen, B. Li, Y. Yang, Z. Li, X. Tan. J. Alloys Compd. **922**, 166174 (2022).
[10] Z. Rao, B. Dutta, F. Körmann, W. Lu, X. Zhou, C. Liu, A. Kwiatkowski da Silva, U. Wiedwald, M. Spasova, M. Farle. Adv. Funct. Mater. **31**, 2007668 (2021).
[11] J. Zhang, X. Wang, X. Li, Y. Zheng, R. Liu, J. Luan, Z. Jiao, C. Dong, P.K. Liaw. Adv. Sci. **9**, *33*, 2203139 (2022).
[12] Z. Li, G. Bai, X. Liu, S. Bandaru, Z. Wu, X.Zhang, M. Yan, H. Xu. J. Alloys Compd. **845**, 156204 (2020),
[13] C. Bazioti, O.M. Løvvik, A. Poulia, P.A. Carvalho, A.S. Azar, P. Mikheenko, S. Diplas, A.E. Gunnas. J. Alloys Compd. **910**, 164724 (2022).
[14] S. Huang, A. Vida, D. Molnar, K. Kadas, L.K. Varga, E. Holmstrom, L. Vitos. Appl. Phys. Lett. **107**, 251906 (2015).
[15] G. Dai, S. Wu, X. Huang. J. Alloys Compd. **902**, 163736 (2022)
[16] L.J. Zhang, K. Guo, H. Tang, M.D. Zhang, J.T. Fan, P. Cui, Y.M. Ma, P.F. Yu, G. Li. Mater. Sci. Eng. A**757**, 160 (2019).
[17] W. Ji, W. Wang, H. Wang, J. Zhang, Y. Wang, F. Zhang, Z. Fu. Intermetallics **56**, 24 (2015).
[18] M.D. Alcala, C. Real, I. Fombella, I. Trigo, J.M. Cordoba. J. Alloys Compd. **749**, 834 (2018).
[19] N.I. Kourov, V.G. Pushin, A.V. Korolev, Yu.V. Knyazev, N.N. Kuranova, M.V. Ivchenko, Yu.M. Ustuygov, N. Vanderka. Physics of the Solid State **57**, *8*, 1579 (2015). (in Russian).
[20] R.K. Mishra, R.R. Shahi. Magnetis Magnetic Materials / Ed. N. Panwar. InTech. (2018).
[21] S.S. Djokic, Ž. Antić, N.S. Djokic, T. Thundat. J. Serb. Chem. Soc. **84**, *11*, 1199 (2019).
[22] D.A. Velikanov. Vestn. SibGAU **53**, *1*, 147 (2014). (in Russian).
[23] R.S. Iskhakov, S.V. Komogortsev. Phys. Met. Metallogr. **112**, 666 (2011).
[24] R.S. Iskhakov, L.A. Kuzovnikova, S.V. Komogortsev, E.A. Denisova, A.D. Balaev, G.N. Bondarenko. Phys. Met. Metallogr. **102**, *Suppl. 1*, S64 (2006).
[25] S. Guo, C.T. Liu. Prog. Nature. Sci.: Mater. Int. **21**, *6*, 433 (2011).
[26] A.D. Pogrebnyak, A.A. Bagdasaryan, I.V. Yakuschenko, V.M. Beresnev. Uspekhi khimii **83**, *11*, 1027 (2014). (in Russian).
[27] A. Takeuchi, A. Inoue. Mater. Trans. **46**, *12*, 2817 (2005).
[28] C.C. Tung, J.W. Yeh, T.T. Shun, S.K. Chen, Y.S. Huang, H.C. Chen. Mater. Lett. **61**, *1*, 1 (2007).
[29] C.J. Tong, Y. L. Chen, J.W. Yeh, S.J. Lin, S.K. Chen, T.T. Shun, C.H. Tsau, S.Y. Chang. Met. Mater. Trans. A**36**, 881 (2005).
[30] S. Guo, C. Ng, J. Lu, C.T. Liu. J. Appl. Phys. **109**, 103505 (2011).
[31] Z. Rao, A. Çakır, Ö. Özgün, D. Ponge, D. Raabe, Z. Li, M. Acet. Phys. Rev. Materials **5**, 044406 (2021).

Translated by T.Zorina